BIOIMPEDANCE

SVERRE GRIMNES
ØRJAN G. MARTINSEN
University of Oslo
Oslo, Norway

Bioimpedance describes the passive electrical properties of biological materials and serves as an indirect transducing mechanism for physiological events, often in cases where no specific transducer for that event exists. It is an elegantly simple technique that requires only the application of two or more electrodes. According to Geddes and Baker (1), the impedance between the electrodes may reflect "seasonal variations, blood flow, cardiac activity, respired volume, bladder, blood and kidney volumes, uterine contractions, nervous activity, the galvanic skin reflex, the volume of blood cells, clotting, blood pressure and salivation."

Impedance $\boldsymbol{Z}$ [ohm, Ω] is a general term related to the ability to oppose ac current flow, expressed as the ratio between an ac sinusoidal voltage and an ac sinusoidal current in an electric circuit. Impedance is a complex quantity because a biomaterial, in addition to opposing current flow, phase-shifts the voltage with respect to the current in the time-domain. *Admittance* $\boldsymbol{Y}$ [siemens, S] is the inverse of impedance ($\boldsymbol{Y} = 1/\boldsymbol{Z}$). The common term for impedance and admittance is *immittance* (2).

The conductivity of the body is ionic (electrolytic), because of for instance Na^+ and Cl^- in the body liquids. The ionic current flow is quite different from the electronic conduction found in metals: Ionic current is accompanied by substance flow. This transport of substance leads to concentrational changes in the liquid: locally near the electrodes (electrode polarization), and in a closed-tissue volume during prolonged dc current flow.

The studied *biomaterial* may be living tissue, dead tissue, or organic material related to any living organism such as a human, animal, cell, microbe, or plant. In this chapter, we will limit our description to human body tissue.

Tissue is composed of cells with poorly conducting, thin-cell membranes; therefore, tissue has capacitive properties: the higher the frequency, the lower the impedance. Bioimpedance is frequency-dependent, and impedance *spectroscopy*, hence, gives important information about tissue and membrane structures as well as intra- and extracellular liquid distributions. As a result of these capacitive properties, tissue may also be regarded as a *dielectric* (3). Emphasis is then shifted to ac *permittivity* (ε) and ac losses. In linear systems, the description by permittivity or immittivity contains the same information. It must also be realized that permittivity and immittivity are *material constants*, whereas immittance is the directly measured quantity dependent on tissue and electrode geometries. In a heterogeneous biomaterial, it is impossible to go directly from a measured immittance spectrum to the immittivity distribution in the material. An important challenge in the bioimpedance area is to base data interpretation on a better knowledge of the immittivity of the smaller tissue components (2–11).

1. TYPICAL BIOIMPEDANCE DATA

Figure 1 shows the three most common electrode systems. With two electrodes, the current carrying electrodes and signal pick-up electrodes are the same (Fig. 1, left). If the electrodes are equal, it is called a bipolar lead, in contrast to a monopolar lead. With 3-(tetrapolar) or 4-(quadropolar) electrode systems, separate current carrying and signal pick-up electrodes exist. The impedance is then *transfer* impedance (12): The signal is not picked up from the sites of current application.

The 4-electrode system (Fig. 1, right) has separate pick-up (PU) and current carrying (CC) electrodes. With ideal voltage amplifiers, the PU electrodes are not current carrying, and therefore, their polarization impedances do not introduce any voltage drop disturbing measured tissue impedance. In the 3-electrode system (Fig. 1, middle), the measuring electrode M is both a CC and signal PU electrode.

1.1. A 4-Electrode Impedance Spectrum

Figure 2 shows a typical transfer impedance spectrum (Bode plot) obtained with the 4-electrode system of Fig. 1 (right). It shows two *dispersions* (to be explained later). The transfer impedance is related to, but not solely determined by, the arm segment between the PU electrodes. As we shall see, the spectrum is determined by the sensitivity field of the 4-electrode system as a whole. The larger the spacing between the electrodes, the more the results are determined by deeper tissue volumes. Even if all the electrodes are skin surface electrodes, the spectrum is, in principle, not influenced by skin impedance or electrode polarization impedance.

For many, it is a surprise that the immittance measured will be the same if the CC and PU electrodes are interchanged (the reciprocity theorem).

1.2. A 3-Electrode Impedance Spectrum

Figure 3 shows a typical impedance spectrum obtained with three skin surface electrodes on the underarm (Fig.

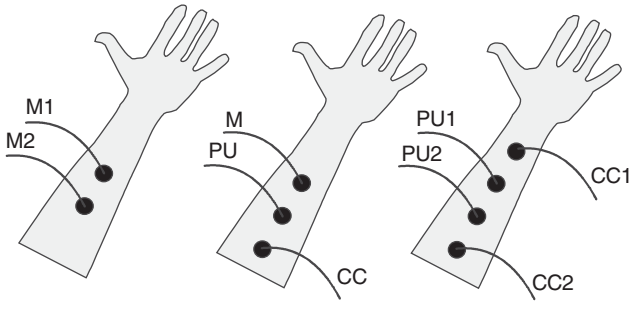

Figure 1. Three skin surface electrode systems on an underarm. Functions: M = measuring and current carrying, CC = current carrying, PU = signal pick-up.

1, middle). Notice the much higher impedance levels than found with the 4-electrode system. The measured zone is under M and comprises electrode polarization, skin impedance, and deeper layer impedance, all physically in series. The electrode polarization impedance is a source of error; electrode impedance is not tissue impedance. At low frequencies (< 1000 Hz), the result is dominated by the high impedance of the human skin with negligible influence from the polarization impedance of the electrode. At high frequencies (> 100 kHz), the results are dominated by deeper layer tissues.

Figure 3 also shows the effect of contact electrolyte penetration into the initially dry skin (three curves: at the moment of electrode onset on dry skin, after 1 h, and after 4 h). The electrode polarization contribution can be judged by studying Fig. 11. Initially, the electrode polarization impedance has negligible influence on the LF results; however, at HF, around 20% of the measured impedance is from the M electrode itself.

Also, the immittance measured will be the same if the CC and PU electrodes are interchanged (the reciprocity theorem).

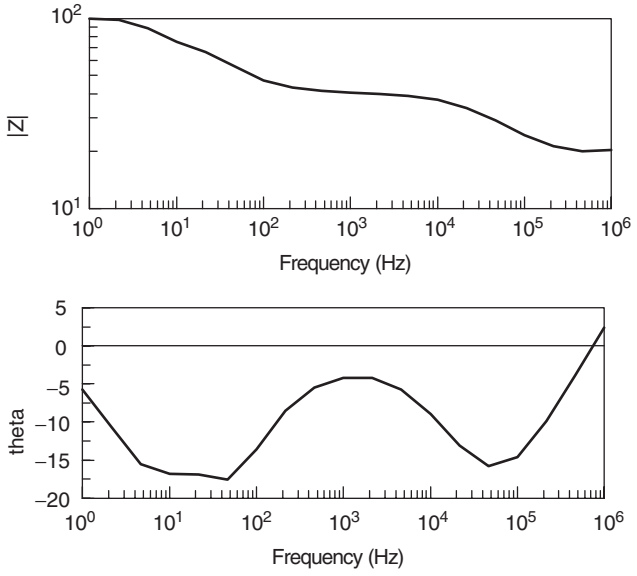

Figure 2. Typical impedance spectrum obtained with four equal electrodes attached to the skin of the underarm as shown on Fig. 1 (right). All electrodes are pregelled ECG-electrodes with skin gel-wetted area 3 cm^2. Distance between electrode centers: 4 cm.

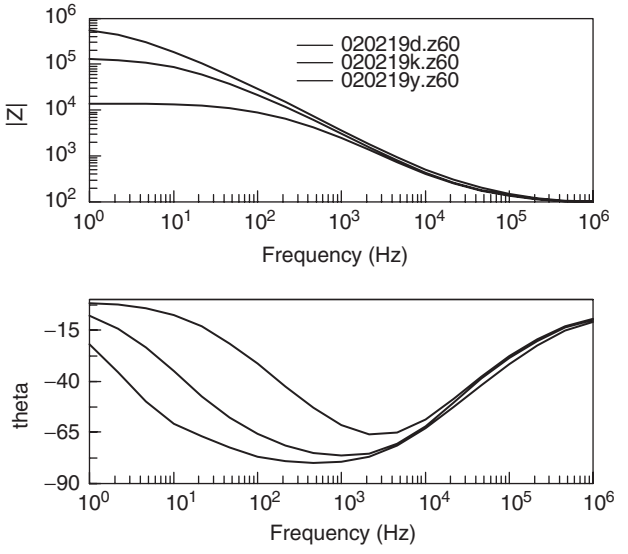

Figure 3. Typical impedance spectrum obtained with the 3-electrode system on the underarm as shown on Fig. 1 (middle). The parameters are: at the time of electrode onset on dry skin, after 1 h, and after 4 h of contact.

2. FROM MAXWELL TO BIOIMPEDANCE EQUATIONS

The Maxwell equation most relevant to bioimpedance is:

$$\nabla \times \boldsymbol{H} - \partial \boldsymbol{D}/\partial t = \boldsymbol{J} \tag{1}$$

$$\boldsymbol{D} = \varepsilon_o \boldsymbol{E} + \boldsymbol{P} \tag{2}$$

where $\boldsymbol{H}$ = magnetic field strength [A/m], $\boldsymbol{D}$ = electric flux density [coulomb/m^2], $\boldsymbol{J}$ = current density [A/m^2], $\boldsymbol{E}$ = electric field strength [V/m], ε_o = permittivity of vacuum [farad (F) /m], and $\boldsymbol{P}$ = electric polarization, dipole moment pr. volume [coulomb/m^2].

If the magnetic component is ignored, Equation 1 is reduced to:

$$\partial \boldsymbol{D}/\partial t = -\boldsymbol{J} \tag{3}$$

Equations 1–3 are extremely robust and also valid under *nonhomogeneous, nonlinear, and anisotropic* conditions. They relate the time and space derivatives at a point to the current density at that point.

Impedance and permittivity in their simplest forms are based on a basic capacitor model (Fig. 4) and the introduction of some restrictions:

a) Use of sufficiently small voltage amplitude v across the material so the system is *linear*. b) Use of *sinusoidal* functions so that with complex notation a derivative (e.g., $\partial \boldsymbol{E}/\partial t$) is simply the product $j\omega \boldsymbol{E}$ (j is the imaginary unit and ω the angular frequency). c) Use of $\boldsymbol{D} = \varepsilon \boldsymbol{E}$ (space vectors), where the permittivity $\varepsilon = \varepsilon_r \varepsilon_o$, which implies that $\boldsymbol{D}$, $\boldsymbol{P}$, and $\boldsymbol{E}$ all have the same direction, and therefore, that the dielectric is considered isotropic. d) No fringe effects in the capacitor model of Fig. 4.

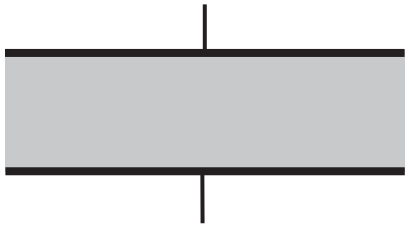

Figure 4. The basic capacitor model.

Under these conditions, a lossy dielectric can be characterized by a complex dielectric constant $\boldsymbol{\varepsilon} = \varepsilon' - j\varepsilon''$ or a complex conductivity $\boldsymbol{\sigma} = \sigma' + j\sigma''$ [S/m], then $\sigma' = \omega\varepsilon''$ (2). Let us apply Equation 3 on the capacitor model where the metal area is $\boldsymbol{A}$ and the dielectric thickness is $\boldsymbol{L}$. However, Equation 3 is in differential form, and the interface between the metal and the dielectric represents a discontinuity. Gauss law as an integral form must therefore be used, and we imagine a thin volume straddling an area of the interface. According to Gauss law, the outward flux of D from this volume is equal to the enclosed free charge density on the surface of the metal. With an applied voltage v, it can be shown that $D = v\varepsilon/L$. By using Equation 3, we then have $\partial D/\partial t = j\omega v\varepsilon/L = J$, and $i = j\omega v\varepsilon A/L = vj\omega C$.

We now leave the dielectric and take a look at the external circuit where the current $\boldsymbol{i}$ and the voltage $\boldsymbol{v}$ (time vectors) are measured and the immittance determined. The admittance is $\boldsymbol{Y} = \boldsymbol{i}/\boldsymbol{v}$ [siemens, S]. With no losses in the capacitor, $\boldsymbol{i}$ and $\boldsymbol{v}$ will be phase-shifted by 90° (the quadrature part). The conductance is $G = \sigma' A/L$ [S], and the basic equation of bioimpedance is then (time vectors):

$$\boldsymbol{Y} = G + j\omega C \tag{4}$$

Three important points must be made here:

First, Equation 4 shows that the basic impedance model actually is an *admittance* model. The conductive and capacitive (quadrature) parts are physically in parallel in the model of Fig. 4.

Second, the model of Fig. 4 is predominantly a dielectric model with *dry* samples. In bioimpedance theory, the materials are considered to be *wet*, with double layer and polarization effects at the metal surfaces. Errors are introduced, which, however, can be reduced by introducing 3- or 4-electrode systems (Fig. 1). Accordingly, in dielectric theory, the dielectric is considered as an *insulator* with dielectric losses; in bioimpedance theory, the material is considered as a *conductor* with capacitive properties. Dry samples can easily be measured with a 2-electrode system. Wet, ionic samples are prone to errors and special precautions must be taken.

Third, Equations 1–3 are valid at a point. With a homogeneous and isotropic material in Fig. 4, they have the same values all over the sample. With inhomogeneous and anisotropic materials, the capacitor model implies values averaged over the volume. Then, under *linear* (small signal) conditions, Equation 4 is still correct, but the measured values are difficult to interpret. The capacitor is basically an *in vitro* model with a biomaterial placed in the measuring chamber. The average anisotropy can be measured by repositioning the sample in the capacitor. *In vivo* measurements, as shown in Fig. 1, must be analyzed from sensitivity fields, as shown in the next chapter.

From Equation 3, the following relationship is easily deduced (space vectors):

$$\boldsymbol{J} = \sigma \boldsymbol{E}. \tag{5}$$

Equation 5 is not valid in anisotropic materials if σ is a scalar. Tissue, as a rule, is anisotropic. Plonsey and Barr (5) discussed some important complications posed by tissue anisotropy and also emphasized the necessity of introducing the concept of the *bidomain*. A bidomain model is useful for cardiac tissue, where the cells are connected by two different types of junctions: tight junctions and gap junctions where the interiors of the cells are directly connected. The intracellular space is one domain and the interstitial space the other domain.

3. GEOMETRY, SENSITIVITY AND RECIPROCITY

Resistivity ρ [$\Omega \cdot$ m] and *conductivity* σ [S/m] are *material constants* and can be extended to their complex analogues: impedivity [$\Omega \cdot$ m] and admittivity [S/m]. The resistance of a cylinder volume with length L, cross-sectional area A, and uniform resistivity ρ is:

$$R = \rho L/A. \tag{6}$$

Equation 6 shows how bioimpedance can be used for volume measurements (plethysmography). Notice, however, that, for example, a resistance increase can be caused either by an increased tissue length, a reduced cross-sectional area, or an increased resistivity. Tissue dielectric and immittivity data are listed by Duck (13).

Figure 5 illustrates typical resistance values for body segments (2), valid without skin contribution and without current constrictional effects caused by small electrodes. By using the term "resistance," we indicate that they are not very frequency-dependent. Notice the low resistance of

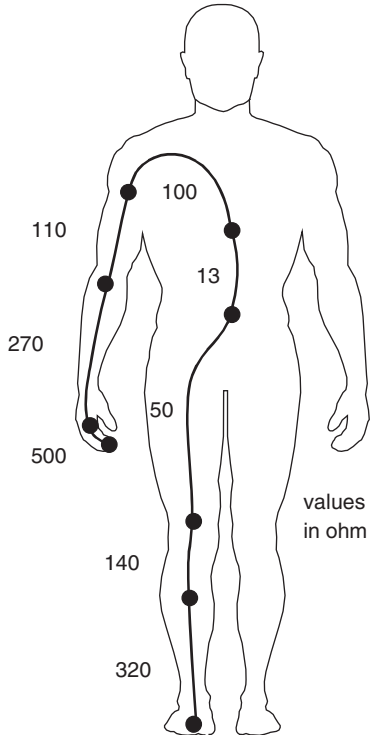

Figure 5. Typical body segment resistance values. From (2), by permission.

the thorax (13 Ω) and the high resistance of one finger (500 Ω).

Figure 6 shows the effect of a constrictional zone caused by one small electrode. Such an electrode system is called *monopolar* because most of the measuring results are a result of the impedance of the small electrode proximity zone.

3.1. Sensitivity Field of an Electrode System

Intuitively, it is easy to believe that if a small tissue volume changes immittivity, the influence on the measurement result is larger the nearer that tissue volume is to the electrodes, which is indeed the case and is illustrated by an equation based on the work of Geselowitz (14):

$$R = \int_V \rho \boldsymbol{J}_{CC} \cdot \boldsymbol{J}_{reci} dv, \tag{7}$$

where R is the transfer resistance [Ω] measured by a 4-electrode system; ρ is the local resistivity in the small volume dv (if ρ is complex, the integral is the transfer impedance $\boldsymbol{Z}$); $\boldsymbol{J}_{CC}$ [1/m^2] is the local current density space vector in dv caused by the CC electrodes carrying a *unity* current; and $\boldsymbol{J}_{reci}$ [1/m^2] is the local current density space vector in dv caused by the PU electrodes *if they also carried a unity current* (reciprocal excitation).

The product $\boldsymbol{J}_{CC} \cdot \boldsymbol{J}_{reci}$ is the local dot vector product, which may be called the local *sensitivity* S [1/m^4] of the electrode system:

$$S = \boldsymbol{J}_{CC} \cdot \boldsymbol{J}_{reci}. \tag{8}$$

Unity current is used so that sensitivity is a purely geometrical parameter not dependent on any actual current level. S is a scalar with positive or negative values in different parts of the tissue; the spatial distribution of S is the *sensitivity field*.

The implications of Equation 7 are important, and at first sight counter intuitive: In a 4-electrode system, *both* electrode pairs determine the sensitivity, not just the PU electrodes as one may intuitively believe. There will be zones of negative sensitivity in the tissue volume between the PU and CC electrodes. The zones will be dependent on, for example, the distance between the PU and CC electrodes. The PU and CC current density fields enter Equation 7 in the same way, and the interchange of the PU and CC electrodes do not change the value of R. Equation 7 is therefore based on the *reciprocity* theorem (14).

In a monopolar or bipolar electrode system, Equation 7 simplifies to

$$R = \int_V \rho \boldsymbol{J}^2 dv \quad S = \boldsymbol{J}^2, \tag{9}$$

where $\boldsymbol{J}$ [1/m^2] is the local current density caused by a unity current passed through the electrode pair.

The analysis of the sensitivity field of an electrode system is of vital importance for the interpretation of measured immittance. Figure 7 (top) illustrates, for instance, the effect of electrode dimensions in a bipolar electrode system. As the gap between the electrodes narrows, the local sensitivity in the gap increases according to $S = \boldsymbol{J}^2$. However, the volume of the gap zone also becomes smaller, and the overall contribution to the integral of Equation 7 is not necessarily dominating. If local changes (e.g., from a pulsating blood artery) is to be picked up, the artery should be placed in such a high-sensitivity zone.

Figure 7 (bottom) illustrates the effect of electrode-electrode center distance in a bipolar system. As distance is increased, the sensitivity in deeper layers will increase but still be small. However, large volumes in the deeper layers will then have a noticeable effect, as small volumes proximal to the electrodes also have.

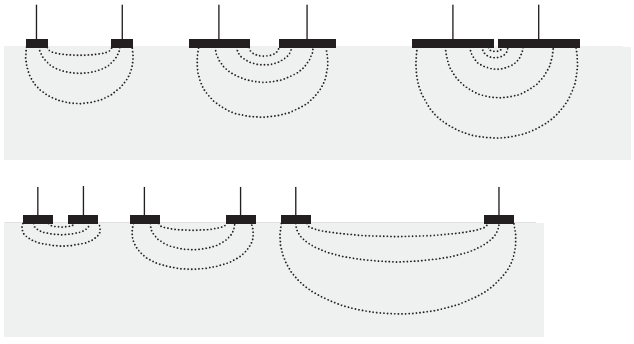

Figure 7. The measuring depth as a function of electrode dimensions (top) and electrode spacing (bottom). From (2), by permission.

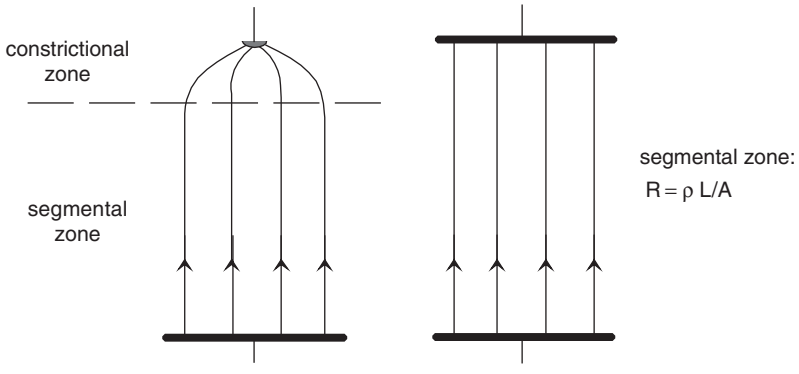

Figure 6. Left: Monopolar system with one electrode much smaller than the other. Increased resistance from the constrictional current zone with increased current density. Right: Segment resistance with uniform current density, large bipolar electrodes. From (2), by permission.

4. ELECTRICAL MODELS

Bioimpedance is a measure of the passive properties of tissue, and, as a starting point, we state that tissue has resistive and capacitive properties showing relaxation, but not resonance, phenomena. As shown by Equation 4, *admittance* is

$$\boldsymbol{Y} = G + j\omega C_p$$

$$\varphi = \arctan(\omega C_p / G)$$

$$|\boldsymbol{Y}|^2 = G^2 + (\omega C_p)^2, \tag{10}$$

where φ is the phase angle indicating to what extent the voltage is time-delayed, G is the parallel conductance [S], and C_p the parallel capacitance [F].

The term ωC_p is the capacitive *susceptance*.

Impedance is the inverse of admittance ($\boldsymbol{Z} = 1/\boldsymbol{Y}$); the equations are:

$$\boldsymbol{Z} = R - j/\omega C_s$$

$$\varphi = \arctan(-1/\omega R C_s)$$

$$|\boldsymbol{Z}|^2 = R^2 + (1/\omega C_s)^2. \tag{11}$$

The term $-1/\omega C_s$ is the capacitive *reactance*.

The values of the series (R_s, C_s) components values are not equal to the parallel ($1/G$, C_p) values:

$$\boldsymbol{Z} = R_s - j/\omega C_s = G/|\boldsymbol{Y}|^2 - j\omega C_p/|\boldsymbol{Y}|^2. \tag{12}$$

Equation 12 illustrates the serious problem of choosing, for example, an impedance model if the components are physically in parallel: R_s and C_s are both frequency-dependent when G and C_p are not. Implicit in these equations is the notion that impedance is a series circuit of a resistor and a capacitor, and admittance is a parallel circuit of a resistor and a capacitor. Measurement results must be given according to one of these models. A model must be chosen, no computer system should make that choice. An important basis for a good choice of model is deep knowledge about the system to be modeled. An electrical model is an electric circuit constituting a substitute for the real system under investigation, as an equivalent circuit.

One ideal resistor and one ideal capacitor can represent the measuring results on one frequency, but can hardly be expected to mimic the whole immittance spectrum actually found with tissue. Usually, a second resistor is added to the equivalent circuit, and one simple and often surprisingly effective addition is also to replace the capacitor C by a more general CPE (Constant Phase Element). A CPE is not a physical device but a mathematical model, you cannot buy a CPE as you buy a resistor ($\varphi = 0^\circ$) or a capacitor ($\varphi = 90^\circ$). A CPE can have any constant phase angle value between 0° and 90°, and mathematically, it is a very simple device (2). Figure 8 shows a popular equivalent circuit in two variants.

One such circuit defines *one dispersion* (15), characterized by two levels at HF and LF, with a transition zone where the impedance is complex. Both at HF ($\boldsymbol{Z} = R_\infty$) and at LF ($\boldsymbol{Z} = R + 1/G_{\text{var}}$), the impedance $\boldsymbol{Z}$ is purely resistive, determined by the two ideal resistors. The circuit of Fig. 8 (left) is with three ideal, frequency-independent components, often referred to as the Debye case, and the impedance is:

$$\boldsymbol{Z} = R_\infty + \frac{1}{G_{\text{var}} + G_{\text{var}} j\omega\tau} \quad \tau = C/G_{\text{var}}.$$

The diagram to the right in Fig. 8 is with the same two ideal resistors, but the capacitor has been replaced by a CPE (2). The equivalent circuit of a CPE consists of a resistor and a capacitor, both frequency-dependent so that the phase becomes frequency-independent.

$$\boldsymbol{Z} = R_\infty + \frac{1}{G_{\text{var}} + G_1 (j\omega\tau)^\alpha}$$

$$j^\alpha = \cos(\alpha\pi/2) + j\,\sin(\alpha\pi/2) \tag{13}$$

In Equation 13, the CPE admittance is $G_1(j\omega\tau)^\alpha$; and τ may be regarded as a mean time constant of a tissue volume with a distribution of different local time constants. τ may also be regarded just as a frequency scaling factor; $\omega\tau$ is dimensionless and G_1 is the admittance value at the characteristic angular frequency when $\omega\tau = 1$. α is related both to the constant phase φ of the CPE according to j^α and $\varphi = \alpha \cdot 90^\circ$ and to the frequency exponent in the term ω^α. This double influence of α presupposes that the system is Fricke-compatible. According to Fricke's law, the phase angle φ and the frequency exponent m are related in many electrolytic systems so that $\varphi = \mathrm{m} \cdot 90^\circ$. In such cases, m is replaced by α (2,16).

A less general version of Equation 13 was given by Cole (17):

$$\boldsymbol{Z} = R_\infty + \frac{\Delta R}{1 + (j\omega\tau)^\alpha} = R_\infty + \frac{1}{\Delta G + \Delta G (j\omega\tau)^\alpha}. \tag{14}$$

The Cole model does not have an independent conductance G_{var} in parallel with the CPE; ΔG controls both the parallel ideal conductance and the CPE, which implies

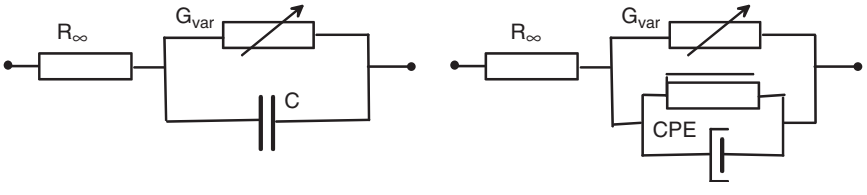

Figure 8. Two versions of a popular equivalent circuit.

that the characteristic frequency is independent of ΔG, in the same way that $\tau = C/G_{var}$ in Equation 11 would be constant if both C and G_{var} varied with the same factor. The lack of an independent conductance variable limits the application of the Cole equation (18). All of Equations 12–14 are represented by circular arc loci if the impedance is plotted in the complex plane, but one of them must be chosen.

Instead of Bode plots, a plot in the complex Argand or Wessel (2) plane may be of value for the interpretation of the results. Figure 9 shows the data of Fig. 2 as a $\boldsymbol{Z}$ and a $\boldsymbol{Y}$ plot. The two dispersions are clearly seen as more or less perfect circular arcs. The LF dispersion is called the α-dispersion, and the HF dispersion is called the β-dispersion (15). β-dispersion is caused by cell membranes and can be modeled with the Maxwell–Wagner structural polarization theory (15,19). The origin of the α-dispersion is more unclear.

Figure 8 is a model well-suited for skin impedance: The R_∞ is the deeper tissue series resistance and the parallel combination represents the stratum corneum with independent sweat duct conductance in parallel. Figure 10 shows another popular model better suited for living tissue and cell suspensions. The parallel conductance G_0 is the extracellular liquid, the capacitance is the cell membranes, and the R is the intracellular contributions.

5. ELECTRODES AND INSTRUMENTATION

The electrode is the site of charge carrier transfer, from electrons to ions or vice versa (20–22). The electrode proper is the contact zone between the electrode metal (electronic conduction) and the electrolyte (ionic conduction). As ionic current implies transport of substance, the electrolytic zone near the metal surface may be depleted or filled with electrolyte species. A double layer will be formed in the electrolyte at the electrode surface. This double layer represents an energy barrier with capacitive properties. Both processes will contribute to electrode polarization immittance. Figure 11 shows the impedance spectrum of a commercial, pregelled ECG electrode of the type used for obtaining the results in Figs. 2 and 3.

5.1. Electrode Designs

Skin surface electrodes are usually made with a certain distance between the metal part and the skin [Fig. 12 (top)]. The enclosed volume is filled with contact electrolyte, often in the form of a gel contained in a sponge. The stronger the contact electrolyte, the more rapid the penetration into the skin. There are two surface areas of concern in a skin surface electrode: The area of contact between the metal and the electrolyte determines the polarization impedance; the electrolyte wetted area of the skin (the effective electrode area, EEA) determines the skin impedance.

Figure 12 (bottom) shows needle electrodes for invasive measurements. Some types are insulated out to the tip; others have a shining metal contact along the needle shaft. Some are of a coaxial type with a thin center lead isolated from the metal shaft.

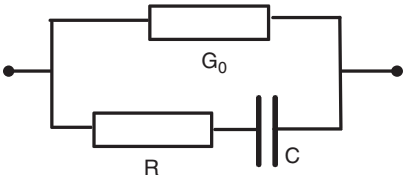

Figure 10. Tissue or suspension equivalent circuit.

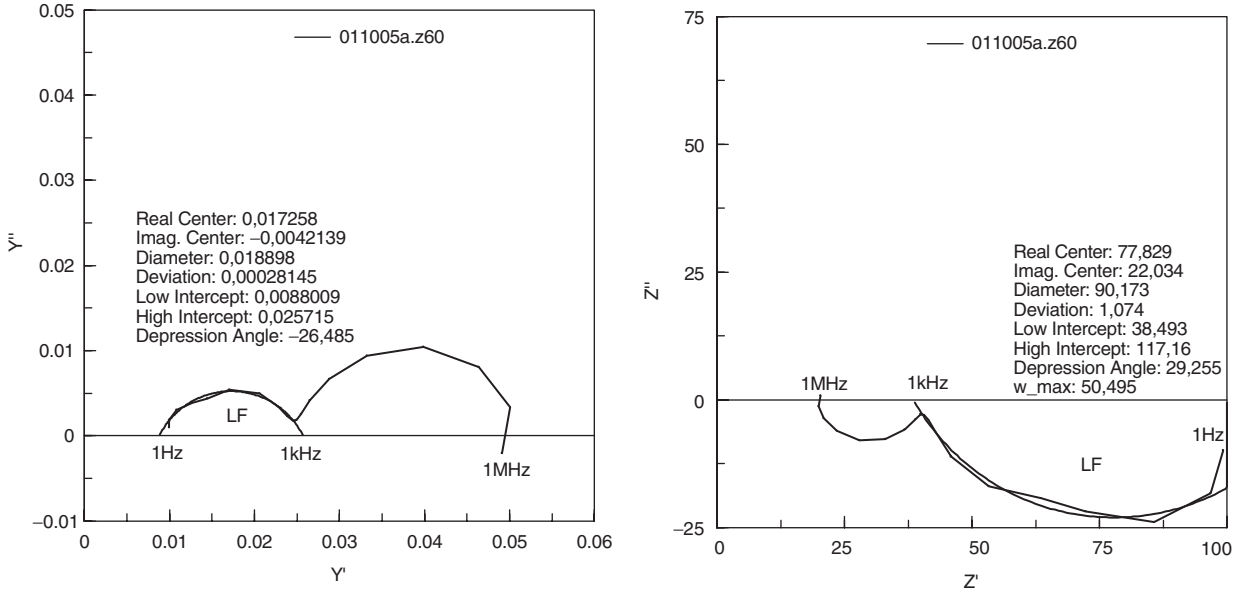

Figure 9. The data in Fig. 2 shown in the complex Wessel diagram as $\boldsymbol{Y}$ and $\boldsymbol{Z}$ plots. Circular arc fits for the same LF dispersion are shown in both plots.

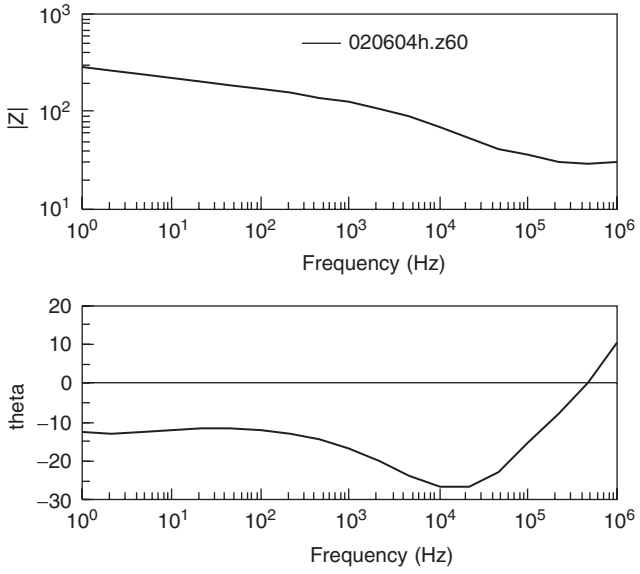

Figure 11. Electrode polarization impedance, one pregelled ECG commercial electrode of the type used in Figs. 2 and 3. The positive phase at HF is caused by the self-inductance of the electrode wire.

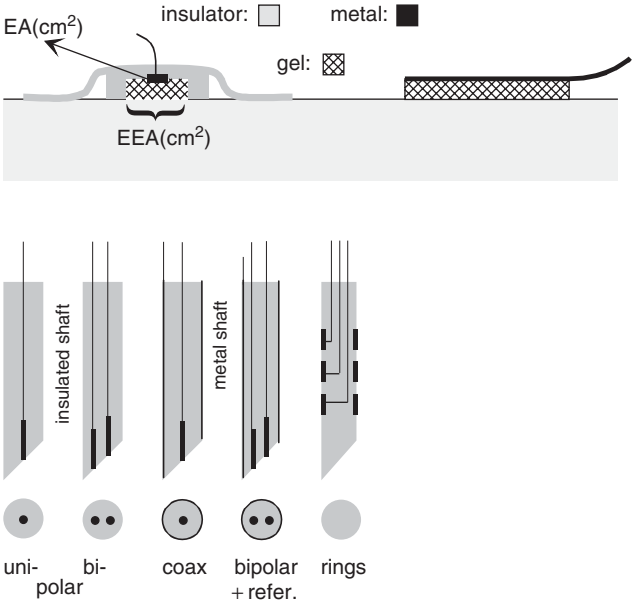

Figure 12. Top: skin surface types. Bottom: invasive needles. From (2), by permission.

With modern technology, it is easy to fabricate microelectrodes with small dots or strips with dimensions in the micrometer range that are well-suited for single-cell discrimination.

5.2. Instrumentation and Software

Bridges achieve high precision. The frequency range is limited (23), although modern self-balanced bridge designs have extended it below 10 Hz. Now, lock-in amplifiers are the preferred instrumentation for bioimpedance measurements (2). The lock-in amplifier needs a synchronizing signal from the signal oscillator for its internal synchronous rectifier. The output of the lock-in amplifier is a signal not only dependent on input signal *amplitude*, but also *phase*. A two-channel lock-in amplifier has two rectifiers synchronous with the in-phase and quadrature oscillator signals. With such an instrument, it is possible to measure complex immittance directly. Examples of commercially available instruments are the SR model series from Stanford Research Systems, the HP4194A, and the Solartron 1260/1294 system with an extended LF coverage (10 μHz–32 MHz). Bioimpedance is measured with small currents so that the system is linear: An applied sine waveform current results in a sine pick-up signal. A stimulating electrode, on the other hand, is used with large currents in the nonlinear region (7), and the impedance concept for such systems must be used with care.

Software for Bode plots and complex plane analysis are commercially available; one example is the Scribner ZView package. This package is well-suited for circular arc fits and equivalent circuit analysis.

5.3. Safety

In a 2- and 3-electrode system, it is usually possible to operate with current levels in the microampere range, corresponding to applied voltages around 10 mV rms. For most applications and direct cardiac, these levels may be safe (24,25).

With 4-electrode systems, the measured voltage for a given current is smaller, and for a given signal-to-noise ratio, the current must be higher, often in the lower mA range. For measuring frequencies below 10 kHz, this is unacceptable for direct cardiac applications. LF mA currents may also result in current perception by neuromuscular excitation in the skin or deeper tissue. Dependent on the current path, these LF current levels are not necessarily dangerous, but are unacceptable for routine applications all the same.

6. SELECTED APPLICATIONS

6.1. Laboratory-on-a-Chip

With microelectrodes in a small sample volume of a cell suspension, it is possible to manipulate, select, and characterize cells by rotation, translocation, and pearl chain formation (26). Some of these processes are monitored by bioimpedance measurements.

6.2. Cell Micromotion Detection

A monopolar microelectrode is convenient to study cell attachment to a surface. Many cell types need an attachment to flourish, and it can be shown that measured impedance is more dominated by the electrode surface the smaller it is. Cell micromotion can be followed with nm resolution on the electrode surface (27).

6.3. Cell Suspensions

The Coulter counter counts single cells and is used in hospitals all over the world. The principle is based on a cell suspension where the cells and the liquid have different impedivities. The suspension is made to flow through a capillary, and the capillary impedance is measured. In addition to rapid cell counting, it is possible to characterize each cell on passing (28).

6.4. Body Composition

Bioimpedance is dependent on the morphology and impedivity of the organs, and with large electrode distances, it is possible to measure segment or total body water, extra- and intracellular fluid balance, muscle mass, and fat mass. Application areas are as diversified as sports medicine, nutritional assessment, and fluid balance in renal dialysis and transplantation. Body composition instruments represent a growing market. Many of them are single-frequency instruments, and with the electrode systems used, it is necessary to analyze what they actually measure (29).

6.5. Impedance Plethysmography

See that entry in this encyclopedia.

6.6. Impedance Cardiography (ICG) and Cardiac Output

A tetrapolar system is used with two band electrodes around the neck, one band electrode corresponding to the apex of the heart, and the fourth further in caudal direction A more practical system uses eight spot electrodes arranged as four double electrodes, each with one PU and one CC electrode. The amplitude of the impedance change $\Delta \boldsymbol{Z}$ as a function of the heartbeat is about 0.5% of the baseline value. The $\Delta \boldsymbol{Z}$ waveform is similar to the aorta blood pressure curve. The *first time derivative* $d\boldsymbol{Z}/dt$ is called the impedance cardiographic curve (ICG). By adding information about patient age, sex, and weight, it is possible to estimate the heart stroke volume and cardiac output. The resistivity of blood is flow-dependent (11), and as long as the origin (heart-, aorta-, lung-filling/emptying) of the signal is unclear, the cardiac output transducing mechanism will also be obscure. Sensitivity field analysis may improve this status (30).

6.7. Skin Moisture

The impedance of the stratum corneum is dependent on its water content. By measuring the skin susceptance, it is possible to avoid the disturbance of the sweat duct parallel conductance (31), and hence assess the hydration state of the stratum corneum. Low-excitation frequency is needed to avoid contribution from deeper, viable skin layers.

6.8. Skin Fingerprint

Electronic fingerprint systems will, in the near future, eliminate the need for keys, pincodes, and access cards in a number of daily-life products. With a microelectrode matrix or array, it is possible to map the fingerprint electrically with high precision using bioimpedance measurements. Live finger detection is also feasible to ensure that the system is not fooled by a fake finger model or a dead finger (32).

6.9. Impedance Tomography

By applying many electrodes on the surface of a body, it is possible to map the distribution of immittivity in the volume under the electrodes (33–35). One approach is to use, for example, 16 electrodes, excite one pair and arrange a multichannel measurement of the transfer impedance in all the other unexcited pairs (Fig. 13). By letting all pairs be excited in succession, one complete measurement is performed. By choosing a high measuring frequency of, for example, 50 kHz, it is possible to sample data for one complete image in less than one tenth of a second, and live images are possible. The sensitivity in Equation 9 clearly shows that it is more difficult to obtain sharp spatial resolution the larger the depth from the skin surface. In practice, the resolution is on the order of centimeters; therefore, other advantages are pursued (e.g., the instrumentation robustness and the simplicity of the sensors).

6.10. Monitoring Tissue Ischemia and Death

Large changes in tissue impedance occur during ischemia (36,37), tissue death, and the first hours afterward (2). The changes are related to changed distribution of intracellular and extracellular liquids, variations in the gap junctions between the cells, and, in the end, the breakdown of membrane structures.

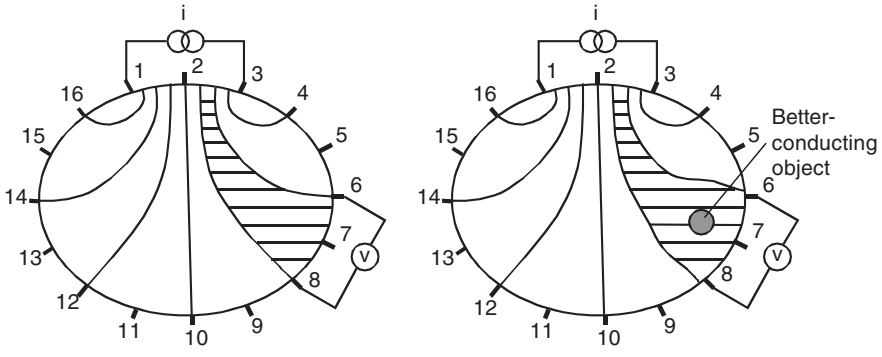

Figure 13. Principle of a tomography setup. From (2), by permission.

7. FUTURE TRENDS

Basic scientific topics: immittivity of the smaller tissue components, sensitivity field theory, impedance spectroscopy and tissue characterization, nonlinear tissue properties, and single-cell manipulation.

Instrumentation: ASIC (Application Specific Integrated Circuit) design as a new basis for small and low-cost instrumentation, also for single-use applications. Telemetry technology to improve signal pick-up and reduce noise and influence from common-mode signals.

Applications: microelectrode technology; single-cell and microbe monitoring; electroporation; electrokinetics (e.g., electrorotation); tissue characterization; monitoring of tissue ablation, tissue/organ state, and death/rejection processes.

BIBLIOGRAPHY

1. L. A. Geddes and L. E. Baker, *Principles of Applied Biomedical Instrumentation*. New York: John Wiley, 1989.
2. S. Grimnes and Ø. G. Martinsen, *Bioimpedance and Bioelectricity Basics*. San Diego, CA: Academic Press, 2000.
3. R. Pethig, *Dielectric and Electronic Properties of Biological Materials*. New York: John Wiley, 1979.
4. S. Ollmar, Methods for information extraction from impedance spectra of biological tissue, in particular skin and oral mucosa—a critical review and suggestions for the future. *Bioelectrochem. Bioenerg*. 1998; **45**:157–160.
5. R. Plonsey and R. C. Barr, A critique of impedance measurements in cardiac tissue. *Ann. Biomed. Eng*. 1986; **14**:307–322.
6. J. Malmivuo and R. Plonsey, *Bioelectromagnetism*. Oxford, UK: Oxford University Press, 1995.
7. R. Plonsey and R. C. Barr, *Bioelectricity. A Quantitative Approach*. New York: Plenum Press, 2000.
8. K. R. Foster and H. P. Schwan, Dielectric properties of tissues and biological materials: a critical review. *CRC Crit. Rev. Biomed. Eng*. 1989; **17**(1):25–104.
9. J.-P. Morucci, M. E. Valentinuzzi, B. Rigaud, C. J. Felice, N. Chauveau, and P.-M. Marsili, Bioelectrical impedance techniques in medicine. *Crit. Rev. Biomed. Eng*. 1996; **24**:223–681.
10. S. Takashima, *Electrical Properties of Biopolymers and Membranes*. New York: Adam Hilger, 1989.
11. K. Sakamoto and H. Kanai, Electrical characteristics of flowing blood. *IEEE Trans. BME* 1979; **26**:686–695.
12. F. F. Kuo, *Network Analysis and Synthesis*, international edition, New York: John Wiley, 1962.
13. F. A. Duck, *Physical Properties of Tissue. A Comprehensive Reference Book*. San Diego, CA: Academic Press, 1990.
14. D. B. Geselowitz, An application of electrocardiographic lead theory to impedance plethysmography. *IEEE Trans. Biomed. Eng*. 1971; **18**:38–41.
15. H. P. Schwan, Electrical properties of tissue and cell suspensions. In: J. H. Lawrence and C. A. Tobias, eds., *Advances in Biological and Medical Physics*, vol. V. San Diego, CA: Academic Press, 1957, pp. 147–209.
16. H. Fricke, Theory of electrolytic polarisation. *Phil. Mag*. 1932; **14**:310–318.
17. K. S. Cole, Permeability and impermeability of cell membranes for ions. *Cold Spring Harbor Symp. Quant. Biol*. 1940; **8**:110–122.
18. S. Grimnes and Ø. G. Martinsen, Cole electrical impedance model—a critique and an alternative. *IEEE Trans. Biomed. Eng*. 2005; **52**(1):132–135.
19. H. Fricke, The Maxwell–Wagner dispersion in a suspension of ellipsoids. *J. Phys. Chem*. 1953; **57**:934–937.
20. J. R. Macdonald, *Impedance Spectroscopy, Emphasizing Solid Materials and Systems*. New York: John Wiley, 1987.
21. J. Koryta, *Ions, Electrodes and Membranes*. New York: John Wiley, 1991.
22. L. A. Geddes, *Electrodes and the Measurement of Bioelectric Events*. New York: Wiley-Interscience, 1972.
23. H. P. Schwan, Determination of biological impedances. In: W. L. Nastuk, ed., *Physical Techniques in Biological Research*, Vol. 6. San Diego, CA: Academic Press, 1963, pp. 323–406.
24. IEC-60601, Medical electrical equipment. General requirements for safety. International Standard, 1988.
25. C. Polk and E. Postow, eds., *Handbook of Biological Effects of Electromagnetic Fields*. Boca Raton, FL: CRC Press, 1995.
26. R. Pethig, J. P. H. Burt, A. Parton, N. Rizvi, M. S. Talary, and J. A. Tame, Development of biofactory-on-a-chip technology using excimer laser micromachining. *J. Micromech. Microeng*. 1998; **8**:57–63.
27. I. Giaever and C. R. Keese, A morphological biosensor for mammalian cells. *Nature* 1993; **366**:591–592.
28. V. Kachel, Electrical resistance pulse sizing: Coulter sizing. In: M. R. Melamed, T. Lindmo, and M. L. Mendelsohn, eds., *Flow Cytometry and Sorting*. New York: Wiley-Liss Inc., 1990, pp. 45–80.
29. K. R. Foster and H. C. Lukaski, Whole-body impedance—what does it measure? *Am. J. Clin. Nutr*. 1996; **64**(suppl): 388S–396S.
30. P. K. Kaupinen, J. A. Hyttinen, and J. A. Malmivuo, Sensitivity distributions of impedance cardiography using band and spot electrodes analysed by a 3-D computer model. *Ann. Biomed. Eng*. 1998; **26**:694–702.
31. Ø. G. Martinsen and S. Grimnes, On using single frequency electrical measurments for skin hydration assessment. *Innov. Techn. Biol. Med*. 1998; **19**:395–399.
32. Ø. G. Martinsen, S. Grimnes, K. H. Riisnæs, and J. B. Nysæther, Life detection in an electronic fingerprint system. *IFMBE Proc*. 2002; **3**:100–101.
33. K. Boone, Imaging with electricity: report of the European concerted action on impedance tomography. *J. Med. Eng. Tech*. 1997; **21**:6,201–232.
34. P. Riu, J. Rosell, A. Lozano, and R. Pallas-Areny, Multifrequency static imaging in electrical impedance tomography. Part 1: instrumentation requirements. *Med. Biol. Eng. Comput*. 1995; **33**:784–792.
35. J. G. Webster, *Electrical Impedance Tomography*. New York: Adam Hilger, 1990.
36. M. Schaefer, W. Gross, J. Ackemann, M. Mory, and M. M. Gebhard, Monitoring of physiological processes in ischemic heart muscle by using a new tissue model for description of the passive electrical impedance spectra. Proc. 11th Int. Conf. on Electrc. Bioimpedance, Oslo, Norway, 2001: 55–58.
37. M. Osypka and E. Gersing, Tissue impedance and the appropriate frequencies for EIT. *Physiol. Meas*. 1995; **16**:A49–A55.